JOURNAL OF GEOPHYSICAL RESEARCH, VOL. 102, NO. A7, PAGES 14,199–14,207, JULY 1, 1997

Energetics during the main phase of geomagnetic superstorms

R. Monreal Mac-Mahon

Departamento de Matemática y Física, Universidad de Magallanes, Punta Arenas, Chile

W. D. Gonzalez

Divisão de Geofísica Espacial, Instituto de Pesquisas Espaciais, São José dos Campos, Brazil

Abstract. The study of energy transfer between the different regions of the solar wind - magnetosphere - ionosphere system is a fundamental issue in Solar-Terrestrial Physics. In this work we have studied the degradation of the solar wind energy budget through the solar wind - magnetosphere coupling down to the ring current injection and the auroral ionospheric dissipation during the main phase of magnetic superstorms ($Dst < -240$ nT). The interplanetary magnetic field, density, temperature, and solar wind velocity measurements collected by the ISEE 3 satellite, and the total energy flux of high-latitude precipitating particles collected by the NOAA 6 satellite were used for this study. The solar wind energy budget was determined from the kinetic energy flux of the particles in the interplanetary medium. The energy transfer from the solar wind into the magnetosphere was estimated through a dayside magnetopause ram pressure corrected version of the Perrault and Akasofu ϵ function. The energy injection into the ring current was estimated under the DPS theorem restriction and introducing the decay parameter τ in the evolution equation as a continuous function of the Dst index. The energy dissipation estimate in the auroral ionosphere via Joule heating in one hemisphere was computed using ionospheric and interplanetary data through a new method. Previous statistical and case studies for substorms have shown that the total energy dissipated as Joule heating is roughly twice that of the ring current injection. Our results show that the energy dissipation via Joule heating in the auroral ionosphere is about half of the ring current energy injection during superstorms.

1. Introduction

The main goal of this work is the study of the global energetics of the solar wind – magnetosphere system and of its dissipation through the inner magnetosphere during very intense magnetic storms ($Dst < -240$ nT), for which the main dissipation regions are the ring current and the high-latitude ionosphere.

This is the first work that focuses such a study during very intense storms and uses an original method to compute the high-latitude ionospheric dissipation [*Monreal-MacMahon,* 1994], although some results were reported by *Feldstein et al.*[1986] among the study of storms of several intensities. Several previous works [e.g., *Akasofu,* 1981; *Stern,* 1984; *Feldstein et al,* 1990; *Weiss et al,* 1992] have considered relationships between the auroral index AE and the high-latitude ionospheric dissipation during typical active periods, but not during very intense storms. From the events in which we could find full solar wind data coverage, we have chosen the four most intense magnetic storms that have occurred in the space era. Those events laid in the solar maximum neighbourhood of solar cycle 21 with the onsets occurring on December 19, 1980 ($Dst^* = -249$ nT); April 13, 1981 ($Dst^* = 311$ nT); July 13, 1982 ($Dst^* = -325$ nT); September 5, 1982 ($Dst^* = -289$ nT); where Dst^* denotes the peak Dst value including solar wind ram pressure correction [*Gonzalez et al.,* 1989, 1994].

For the same group of "superstorms," *Tsurutani et al.* [1992] studied their solar and interplanetary causes. They concluded that the main cause of these very intense magnetic storms was the high value of the southward interplanetary magnetic field, instead of the intense solar wind speed, related with the interplanetary electric field $E = vB_s$. The correlation between the IMF condition and the activities observed in different points of the magnetosphere have shown that the IMF plays a fundamental role in the energy transport from the solar wind to the magnetosphere and that magnetic reconnection at the magnetopause is the main mechanism, with an efficiency of approximately 10% during intense magnetic storms [*Gonzalez et al.,* 1989].

Paper number 97JA01151.
0148-0227/97/97JA-01151$09.00

The main effect of the interaction between the solar wind and the magnetosphere is the generation of the solar wind - magnetosphere dynamo that can get values up to 10^{11} W in quiet days, up to several 10^{12} W during geomagnetic storms [e.g., *Weiss et al.,* 1992]. In this work we have used the epsilon function [*Perrault and Akasofu,* 1978] and a pressure-corrected expression of it to represent that transfer, and are described in section 2. The main part of the energy produced by that dynamo is injected into the ring current and dissipated in the high-latitude ionosphere via Joule heating, through electric field and current systems. Furthermore, energy deposition through particle precipitation from the plasma sheet and other processes are also involved. The ring current energization and ionospheric Joule heating are studied in section 3. Some case studies are presented in section 4 and the global results in section 5. Finally, section 6 summarizes our conclusions.

2. Solar Wind - Magnetosphere Energy Transfer

The solar wind energy budget is computed from the kinetic energy flux per unit time of particles in the interplanetary medium, namely,

$$U_{sw} = \frac{1}{2}\rho v^3 A, \tag{1}$$

where v and ρ are the velocity and mass density of the solar wind, respectively, and A is the cross section of the dayside magnetopause. As suggested by *Weiss et al.* [1992] we first use L_{CF}^2 for A with $L_{CF} = 30R_E$. As a second step, considering that the radius of the dayside magnetopause depends on the solar wind dynamic pressure, we use R_{CF}^2 for A, where $R_{CF} = (B_0^2/4\pi\rho v^2)^{1/6} R_E$, as obtained from a balance between the kinetic plasma pressure and the magnetic pressure [e.g., *Spreiter et al.,* 1966; *Holzer and Slavin,* 1979; *Sibeck et al.,* 1991], with $B_0 \sim 0.3$ Gauss. Figure 1 shows the profiles of the solar wind kinetic energy flux for days 18 - 20, December 1980 (first event), considering both, constant and pressure corrected magnetopause cross sections. In the bottom panel the Chapman-Ferraro length is shown for this event. The variability in the interplanetary data collected by the ISEE 3 satellite are shown in Figure 2.

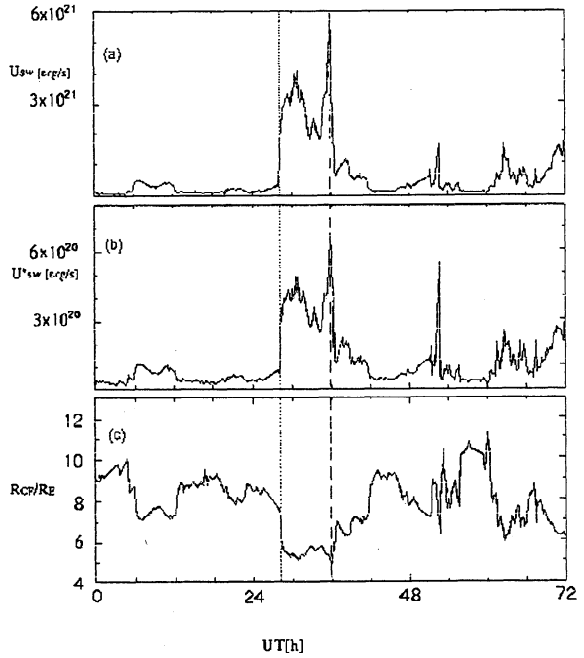

Figure 1. December 18 - 20, 1980. (a) Solar wind kinetic energy rate considering constant cross section (U_{sw}). (b) Solar wind kinetic energy rate considering variable cross section (U_{sw}^*). The bottom panel shows the Chapman-Ferraro scale length in Earth radii. The dotted line during the 19th day shows the interplanetary shock that occurred several hours prior the start of the storm main phase as shown by the dashed line.

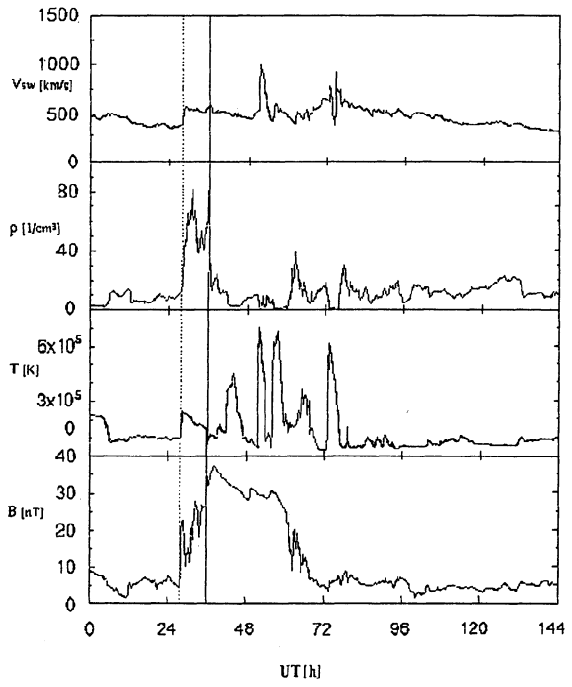

Figure 2. December 18 - 23, 1980. Variability in the interplanetary data collected by the ISEE 3 satellite. The dotted line during the 19th day shows the interplanetary shock that occurred several hours before the start of the storm main phase as shown by the solid line.

The energy transfer from the solar wind into the magnetosphere is determined assuming that reconnection is the responsible process. An estimate of the magnetosphere power entry is the *Perrault and Akasofu* [1978] epsilon coupling function

$$U_m = vB^2 \sin^4(\theta/2) l_0^2, \tag{2}$$

where $l_0 \approx 7R_E$, and a modified, ram pressure corrected, expression is

$$U_m^* = \left(\frac{R_{CF}}{l_0}\right)^2 U_m. \tag{3}$$

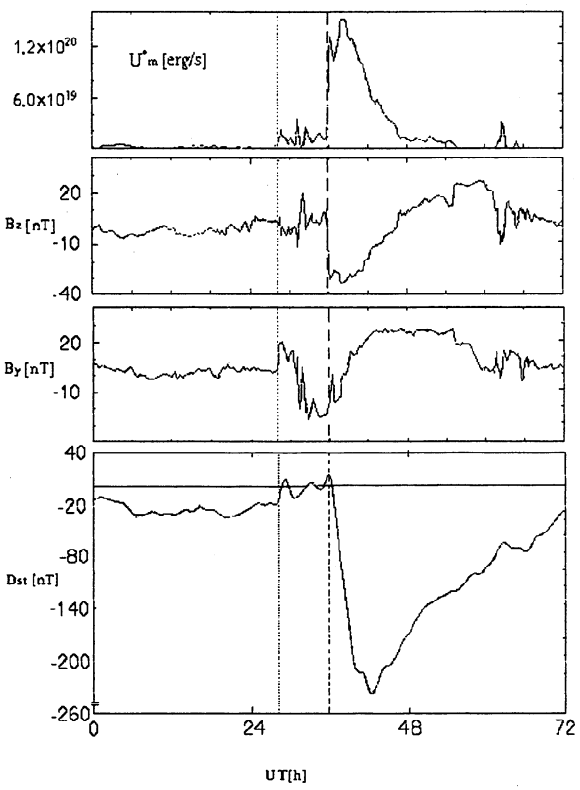

Figure 3. December 18 - 20, 1980. The dotted line marks the abrupt growth in the B_y interplanetary magnetic field component during the interplanetary shock. The dashed line shows the beginning of the magnetic storm main phase together with the abrupt increase in energy transfer into the magnetosphere which is coincident with the steep decreasing slope in the B_z interplanetary magnetic field component. The bottom panel shows the *Dst* index behavior during the same interval of time.

A profile of the energy transfer rate at the magnetopause during the December 1980 event is shown in the first panel of Figure 3, as given by (3).

In the above discussion we note that the use of the expression $L_{CF} = R_{CF}$, to represent the effective magnetospheric cross section - scale length, has at least the physical meaning that it stands for the radius of the dayside magnetopause under pressure balance approximation. On the other hand, the constant values of $L_{CF} = 30\ R_E$ or $l_0 = 7\ R_E$ do not have a physical meaning and have been suggested by *Weiss et al.* [1992] and *Perrault and Akasofu* [1978], respectively, only as ad hoc empirical values. As shown by Figures 1, 2, and 3, by comparing these constant values to those given by the expression for R_{CF}, one can note that 30 R_E is an overstimation, whereas 7 R_E somewhat understimates the magnetosphere scale length for the effective cross section. Thus the residual uncertainties of U_{sw} and of U_m in (1) and (2), respectively, are expected to be around a factor of 4 for the former and a factor of 0.5 for the latter.

The expressions given above for R_{CF}, due to pressure balance, assumes a dipole field approximation for the geomagnetic field. The addition of non-dipole components has led to a modified expression [e.g., *Sibeck et al.*, 1991], which, however, gives values differing typically only by a 10% from those obtained from the simpler expression.

An expression to compute the energy available for redistribution in the inner magnetosphere, which can be compared with (2) and (3) is that worked out by *Gonzalez and Mozer* [1974]:

$$U_{mt} = \frac{4}{\pi}\left(\frac{d_1 d_2 B_I}{R_{mt}}\right)^2 v_{sw}. \tag{4}$$

where d_1 and d_2 are the dawn-dusk and noon-midnight polar ionospheric diameters, B_I is the inferred ionospheric magnetic field, and R_{mt} is the estimated magnetotail radius. This way of computing the energy storage in the magnetotail can be of practical interest because it only needs one interplanetary parameter (the solar wind velocity), which could be obtained, for instance, through interplanetary scintillation [*Hewish,* 1990] if satellite observations in the interplanetary medium are not available. As an example, assuming $R_{mt} = 30\ R_E$, we obtain the following values: 2.1×10^{17} J, 0.98×10^{13} W, and 1.2×10^{13} W, for the energy, mean power and peak power, respectively, during the main phase of the first event. Comparing these values with those of Table 5, one can see that expression (4) provides a reasonable good approach for the energy transferred to the magnetosphere.

3. Ring Current Energy Injection and Ionospheric Dissipation

The particles that move around the Earth forming a ring current at L values around 5 are responsible for the observed ground geomagnetic field decrease. The ring current formation in the inner magnetosphere is thought to be the main consequence of geomagnetic storms [e.g., *Feldstein et al.,* 1990; *Gonzalez et al.,* 1994].

Dessler and Parker [1959] and *Schopke* [1966] showed that the geomagnetic field perturbation in the Earth's surface is related to the total energy of particles K_R by $\Delta B/B_0 = -K_R/K_M$, where $K_M = 8 \times 10^{24}$ ergs is the external geomagnetic field total energy. Thus, the total energy of particles is given by $K_R = 4 \times 10^{20} D$, where D is the pressure corrected *Dst* value, in nanoteslas.

The energy injection rate is obtained from the energy balance equation

$$U_R = 4 \times 10^{20}\left(\frac{dD}{dt} + \frac{D}{\tau}\right) \text{erg/s}, \tag{5}$$

where τ is the particle lifetime in the ring current. To compute U_R it is necessary to know D and τ. Several models for the parameter τ have been used. In a first step it was assumed a constant τ for all possible *Dst* values [e.g., *Burton et al.,* 1975; *Perrault and Akasofu,* 1978; *Murayama,* 1982]. Later it was emphasized the necessity to introduce different τ values for different *Dst* intervals [e.g., *Akasofu,* 1981; *Vasyliunas et al.,* 1982; *Gonzalez et al.,* 1989; *Prigancová and Feldstein,* 1992]. In the present work, to avoid reported discontinuities

determining the ring current energy injection, we use a continuous function for the decay parameter τ that tries to match the empirical models reported previously. The relation is given by

$$\tau = (\alpha/D)^{3/2}, \tag{6}$$

where α is an adjustable parameter. The previous expression holds if we consider that the decay parameter is inversely proportional to cubic power of the ring current's particle velocity.

In (5) and (6) the expression for D involves only ram pressure correction. An additional correction to D due to an internal (solid Earth) source was not taken into account. Such a correction typically reduces the value of D by a factor of 1/3 [e.g., *Gonzalez et al.*, 1994], thus the values obtained from (5) and (6) tend to overstimate U_R.

The global Joule heating rate U_j over the whole polar and auroral region, for one hemisphere, is computed from

$$U_j = \int_0^{\theta_c} \int_0^{2\pi} \Sigma_P E^2 (R_E + h)^2 \sin\theta d\theta d\lambda, \tag{7}$$

where θ_c is the geomagnetic colatitude for the auroral zone-equatorward boundaries, λ is the geomagnetic longitude, and $h = 110$ km is the ionospheric altitude. Σ_P and E are the ionospheric conductance and electric field, respectively.

In order to use the above classical expression [e.g., *Cole*, 1962] it was necessary to compute conductances and electric fields from ionospheric and interplanetary data collected by the NOAA 6 and ISEE 3 satellites, respectively. Figure 4 is a scheme describing briefly our methodology. The Pedersen conductances were calcu-

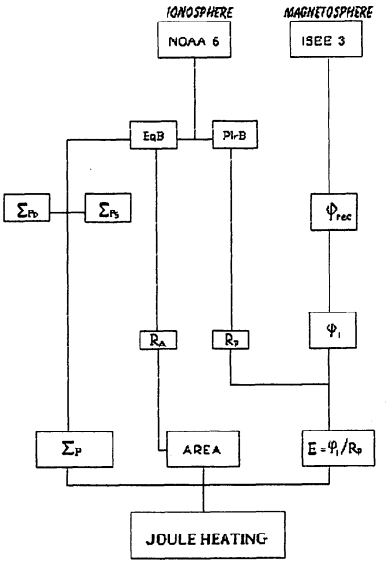

Figure 4. Schematic diagram to compute Joule heating dissipation in the auroral ionosphere. EqB and PlrB are the equatorward and poleward boundaries, respectively. R_a and R_p are the respective auroral and polar radii, ϕ_{rec} is the reconnected electric potential, and ϕ_I is the electric potential in the ionosphere.

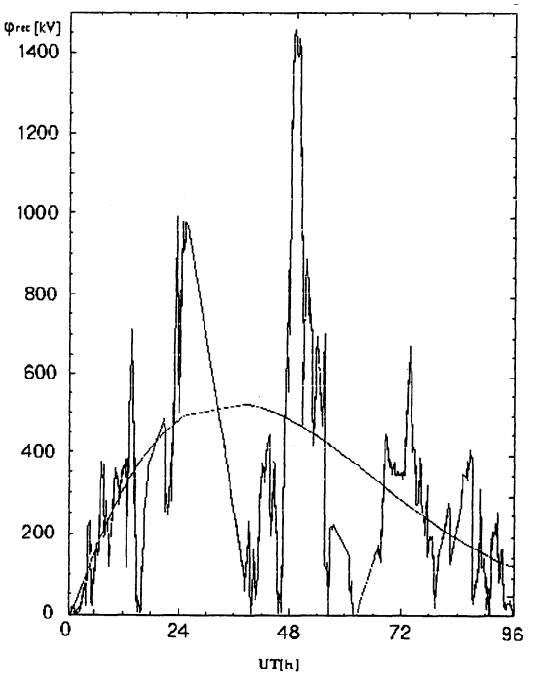

Figure 5. April 11 - 14, 1981. Magnetopause reconnected electric potential computed from interplanetary data. The fitting line is a fifth-order regression curve used to compare with the same regression of the computed AMIE polar ionospheric electric potential (not shown) for the same event. The comparison gives an estimate of the mapping factor.

lated considering contributions of solar light and particle precipitation. The latter contribution based on the precipitation electron model [*Kroehl et al.*, 1988], needs a knowledge of the equatorward boundaries of the auroral zone. From the NOAA satellite we obtained the total energy flux of electrons to determine the equatorward and poleward boundaries. From the equatorward boundaries we estimate the contribution of the precipitating particles (Σ_{Pp}) to the ionospheric conductance which modifies the conductance obtained by considering only the solar radiation (Σ_{Ps}). From both contributions we compute the global Pedersen conductance $\Sigma_P = (\Sigma_{Ps}^2 + \Sigma_{Ps}^2)^{1/2}$. The electric field in the polar ionosphere is estimated in a sort of hybrid way using both ionospheric and interplanetary data. From the ISEE 3 satellite we use the interplanetary data to compute the electric potential due to reconnection [*Gonzalez and Mozer*, 1974] in the magnetopause from which we estimate the mapped ionospheric potential assuming an efficiency factor of 0.3 [*Gonzalez and Mozer*, 1974; *Reiff et al.*, 1986], which was obtained comparing polar cap - ionospheric electric field measurements with reconnection electric models for the magnetopause. A different mapping factor of 0.2 was estimated comparing fifth order regression curves from the magnetopause reconnected potential computed from interplanetary data (Figure 5) and the computed AMIE polar ionospheric electric potential. Once we estimate the ionospheric electric potential ϕ_I we compute the associated electric field $E_I = \phi_I / r_P$, using the polar boundaries determined previously from the ionospheric data. r_P is the

polar radius. Finally the auroral Joule heating dissipation in the ionosphere is estimated from the calculated ionospheric conductance, area and electric field. The results of our methodology were compared with those of the expression found by previous authors [e.g., *Akasofu*, 1981; *Ahn et al.*, 1983; *Stern*, 1984; *Feldstein et al.*, 1990; *Weiss et al.*, 1992], who considered only a linear relationship between the high-latitude geomagnetic index *AE* and the Joule heating dissipation rate. A comparison of the results is given in Table 8.

4. Case Studies

4.1. December 1980

In this event the interplanetary shock identified by the abrupt enhancement in velocity and IMF-intensity (Figure 2) was verified several hours before the incursion of the IMF-B_z component into negative values. Apparently because of this fact the energy available in the solar wind diminishes during the energy transfer time, marked basically by the threshold value $B_z = -10$ nT, reaching small values compared with the energy available in the solar wind during the preceding (shocked) time interval and also in relation to the values found in the other studied superstorms. One can see that small IMF-B_z incursions to negative values previous to the storm main phase already led to some transfer of energy. At the sudden enhancement the magnetopause is strongly compressed, reaching values around $5R_E$ in the Sun-Earth direction (bottom panel of Figure 1). Several hours later, the steep decrease in the B_z component, reaching values around -30 nT, produces a great temporal variation in the *Dst* (bottom panel of Figure 3), as also shown by the largely intensified values of the coupling function (Figure 3).

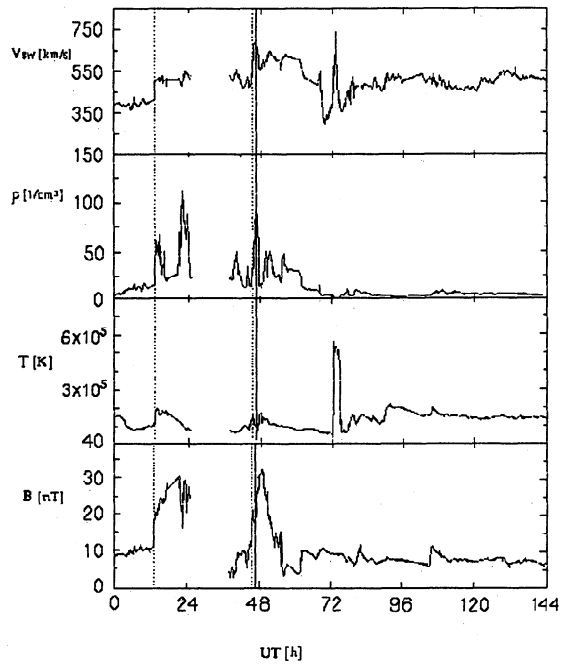

Figure 6. April 11 - 16, 1981. The first three panels show the variability in the interplanetary velocity, density, and temperature data collected by the ISEE 3 satellite and the bottom panel shows IMF intensity. The dotted lines mark interplanetary shocks previous to the beginning of the superstorm main phase shown by the solid line.

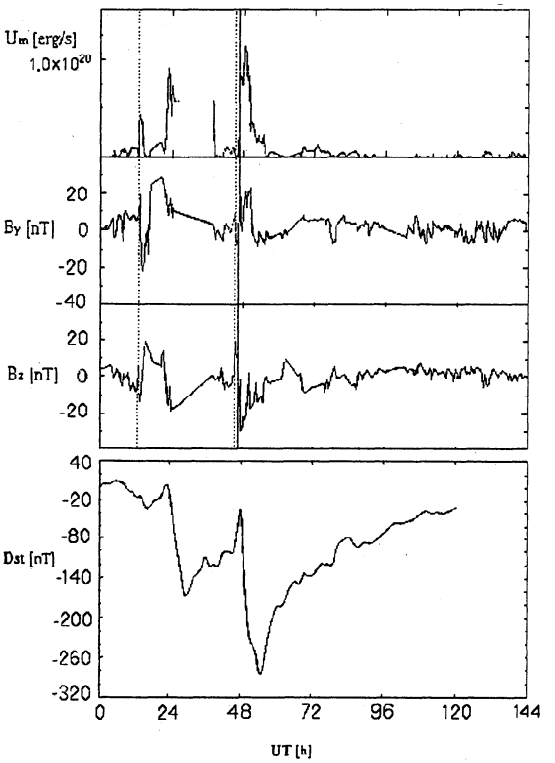

Figure 7. April 11 - 16, 1981. The first panel shows the abrupt increase in energy transfer into the magnetosphere marked by the solid line which is coincident with great variabilities in the interplanetary magnetic field components shown in the following two panels and particularly with the steep decreasing slope in the B_z component. The bottom panel shows the *Dst* index behavior during the same interval of time.

During the storm main phase (approximately 8 hours, with B_z under the threshold value) around 2.5×10^{17} J were transferred into the magnetosphere, with a mean power of approximately 1×10^{13} W. This represents between 15% and 20 % of the solar wind kinetic energy, and it is far over the typical values reported in the literature [*Weiss et al.*, 1992], as well as over the mean values estimated for the other three superstorms. As mentioned above, this large percentage in this case is due to the fact that the kinetic energy of the solar wind is low right at the time interval of the storm's main phase.

4.2. April 1981

In this event the second interplanetary shock shown by the dotted lines in Figures 6 and 7 identified also by the abrupt enhancement in velocity, density and IMF-intensity was verified close to great variabilities in the IMF components and in particular was followed by a steep decrease in the IMF-B_z component which reach negative values as high as -30 nT. The energy trans-

Table 1. Energy, Mean, and Peak Power Available in the Solar Wind

Event	U_{sw}	U^*_{sw}	P_{sw}	P^*_{sw}	E_{sw}	E^*_{sw}
Dec. 19, 1980	75	53	410	180	16	11
April 12, 1981	230	120	720	270	58	30
July 13, 1982	2000	570	4600	1110	590	170
Sept. 6, 1982	540	220	1400	440	110	47
< average >	700	240	1780	500	196	65

E, energy; U, mean power; P, peak power; sw, solar wind. Power in units of 10^{12} W; energy in units of 10^{17} J; asterisk indicates pressure corrected value.

fer into the magnetosphere is meaningful only when $B_S < -10$ nT, as shown by the solid line in Figures 6 and 7. This signature was followed also by the density enhancement and when it abruptly goes down the situation is balanced by an increase in the IMF intensity. When B_z goes over the threshold value and the storm's main phase finishes, the intensity in IMF suddenly diminishes and the solar wind energy transfer into the magnetosphere practically vanishes, in spite of the significative values of the persisting kinetic energy flux.

5. Global Results

The energy and mean power available in the solar wind during the main phase for each event of our study are shown in Table 1. The low values obtained for the event of December 1980 is evident as compared with the other three events. Apparently, only when the IMF-B_z component intrudes to large negative values the effective transfer of energy is triggered into the magnetosphere, even when the kinetic energy available in the solar wind is small, as illustrated by this event.

In the September 1982 event, for which the amount of energy content and mean power in the solar wind occupies the second place in Table 2, the energy transferred into the magnetosphere is the lowest. This is because the B_S peak value is also the lowest and also because the B_z incursion into negative values occurs slowly, reaching values of the order of -20 nT, only after about 5 hours.

Table 2. Transferred to the Magnetosphere

Event	U_m	U^*_m	P_m	P^*_m	E_m	E^*_m
Dec. 19, 1980	120	110	150	130	250	230
April 12, 1981	52	40	110	98	140	110
July 13, 1982	180	59	400	110	520	180
Sept. 6, 1982	42	23	94	75	150	84
< average >	104	61	189	103	260	150

Here m, magnetosphere. Power in units of 10^{11} W; energy in units of 10^{15} J; asterisk indicates pressure corrected value.

Table 3. Percentage Rate Between Energy Transferred to Magnetosphere and Energy Available in the Solar Wind

Event	E^*_m/E_{sw}	E^*_m/E^*_{sw}	E_m/E_{sw}	E_m/E^*_{sw}
April 12, 1981	1.9	3.6	2.2	4.3
July 13, 1982	0.3	1.1	0.9	3.1
Sept. 6, 1982	0.7	1.6	1.3	3.0
< average >	1	2.1	1.5	3.5

Asterisk indicates pressure corrected value.

Rates between the energy available in the solar wind and that transferred into the magnetosphere during the storm's main phase are shown in Tables 3 and 4. The extremely high ratios, between 15% and 20%, resulting on the December 1980 event were disregarded in a first estimate in order to get the average values of Table 3. The ring current injection E_R, mean power U_R, and peak values in power P_R during the storm main phases are shown in Table 5. Again the values obtained during the event of December 1980 are lower than the other events, apparently because the big enhancement in the solar wind pressure that influenced the corrected *Dst* occurred before the main phase. If we assume that approximately half of the energy available in the magnetosphere is dissipated through injection in the ring current and Joule heating in the auroral ionosphere, the ring current injected energy values for the April 1981 and September 1982 appear to be high as compared with the energy transferred to the magnetosphere (Table 6). These high values are probably an overestimation due to the fact that large negative values in the *Dst* index (less than 200 nT) existed during a large part of the main phase, and for which the τ values were mantained below 1 hour. Thus, in Table 6 the numbers in parenthesis were computed modifying the adjustable parameter α ($\alpha_1 = 47 \times 10^3$ nT s$^{2/3}$) such that τ equals one hour when D reaches only 300 nT ($\alpha_2 = 70 \times 10^3$ nT s$^{2/3}$). This suggests that the parameter τ depends not only on D but also on its temporal variation.

The total energy, mean power and peak power values due to dissipation via Joule heating in the auroral iono-

Table 4. Percentage Rate Between Magnetospheric Peak Power and Solar Wind Peak Power

Event	P^*_m/P_{sw}	P^*_m/P^*_{sw}	P_m/P_{sw}	P_m/P^*_{sw}
Dec. 19, 1980	3.2	7.2	3.6	8.3
April 12, 1981	1.4	3.6	1.5	4.1
July 13, 1982	0.24	1.	0.9	3.6
Sept. 6, 1982	0.54	1.7	0.7	2.1
< average >	1.3	3.4	1.7	4.5

Asterisk indicates pressure corrected value.

Table 5. Injection in the Ring Current

Event	U_R	U_R^*	P_R	P_R^*	E_R	E_R^*
Dec 19, 1980	12	8	22	16	25	17
Apr 12, 1981	24	16	46	31	63	41
Jul 13, 1982	30	20	88	61	89	58
Sept 6, 1982	32	24	64	40	67	44
< average >	25	16	52	37	61	40

Power in units of 10^{11} W; energy in units of 10^{15} J; asterisk indicates different adjustable parameter.

Table 7. Dissipation in the Auroral Ionosphere

Event	U_J	U_J^*	P_J	P_J^*	E_J	E_J^*
Dec. 19, 1980	12	9.4	17	13	25	20
April 12, 1981	5.8	4.7	19	16	15	12
July 13, 1982	6.7	4.6	10	8	20	14
Sept. 6, 1982	4.9	4.0	11	9	10	8
< average >	6.9	5.7	14	11.6	18	13.6

Power in units of 10^{11} W; energy in units of 10^{15} J; asterisk indicates different mapping factor.

sphere (one hemisphere), during the main phase of the studied events, are shown in Table 7. In Table 8 we show percentage rates between the ionospheric Joule heating dissipation (for one hemisphere) and the energy transferred to the magnetosphere. The last two columns at the right side of Table 8 were obtained using the empirical linear relationship with the AE index and are used for comparison with our results. For all the events the values computed using the linear relationship are smaller than those calculated with our new method. This was expected due to the underestimation in the auroral index AE during very intense storms. As a result of our estimation it follows that about 16% to 24% of the energy transferred into the magnetosphere is dissipated in the ionosphere (both hemispheres) through Joule heating.

Table 9 shows different sources and sinks in the solar – terrestrial system and their characteristic values of the mean power and integrated energy during the superstorm's main phase. Superstorms with peak B_S values of the order of 25 - 30 nT have main phase durations of approximately 7 hours. From the results shown in Table 9 and summarized in Figure 8, we can visualize a degradation and redistribution of energy during the superstorm main phase. Globally, from the energy available in the solar wind around 1% to 4% is transferred to the magnetosphere. This result is similar to that reported previously in the literature considering smaller storms [e.g., *Weiss et al.*, 1992], but the energy values are larger by a factor of 20 to 80 and the mean power are also 5 to 10 times larger. From the energy available in the magnetosphere among 40% to 65% is distributed in the ring current and the auroral ionosphere, the remaining energy is probably lost through plasmoide ejection and magnetotail heating. The mean power in the ring current injection is $\sim (15-25)\times 10^{11}$ W, whereas the mean ionospheric Joule heat power dissipation is $\sim (11-14)\times 10^{11}$ W. Typical reported values for the ring current power are $\sim 1\times 10^{11}$ W and *Weiss et al.* [1992] suggest that even during very intense storms such power rate could reach only $\sim 6\times 10^{11}$ W. Probably this (subestimated) value resulted from an assumption of using constant τ values of several hours.

6. Conclusions

It was estimated that about 1% and 4% of the energy available in the solar wind is transferred to the magnetosphere during the main phase of superstorms. In average, from the energy transferred to the magnetosphere and available for redistribution in the inner magnetosphere and ionosphere, between 25% and 40% is injected into the ring current and between 16% and 24% is dissipated into the auroral ionosphere.

The energy injected into the ring current was computed using a continuous function of the parameter τ in terms of the pressure corrected Dst index. Our results show that the Joule heating is underestimated when using the linear relation with the AE index during su-

Table 6. Percentage Rate Between Ring Current Injection and Energy Transferred to the Magnetosphere

Event	E_R^*/E_m	E_R^*/E_m^*	E_R/E_m	E_R/E_m^*
Dec. 19, 1980	11 (7.4)	10 (7)	17 (12)	17 (11)
April 12, 1981	57 (37)	45 (29)	47 (32)	42 (28)
July 13, 1982	49 (32)	17 (11)	80 (55)	22 (15)
Sept. 6, 1982	79 (52)	45 (29)	72 (53)	67 (42)
< average >	49 (32)	29 (19)	54 (38)	35 (24)

Quantities between parentheses were computed with a different adjustable parameter as discussed in the text.

Table 8. Percentage Rate Between Ionospheric Joule Heat Dissipation and Energy Transferred to the Magnetosphere

Event	E_J^*/E_m	E_J^*/E_m^*	E_{AE}/E_m	E_{AE}/E_m^*
Dec. 19, 1980	11	10	2	2
April 12, 1981	14	11	5	4
July 13, 1982	11	4	7	3
Sept. 6, 1982	12	7	8	5
< average >	12	8	6	3

E_{AE} ; integral energy value computed using the linear relationship between Joule heat dissipation and AE index.

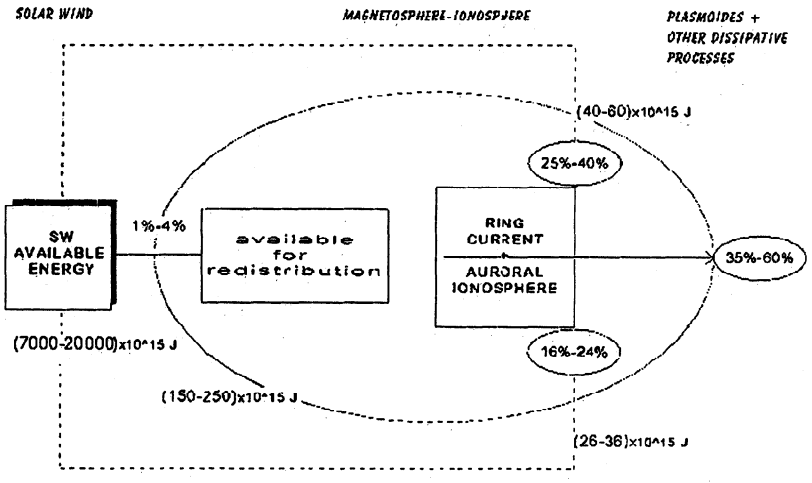

Figure 8. Summary of the energy degradation from the solar wind to the magnetosphere - ionosphere system during the main phase of geomagnetic superstorms ($Dst^* < -240$ nT).

perstorms. On the other hand, the energy dissipation via Joule heating in the auroral ionosphere (both hemispheres) is a little bit over half of the ring current energy injection. The last result contrasts with previous statistical and case studies reported for substorms in which the total energy dissipated as Joule heating is roughly twice that used for the ring current injection.

Thus, in our opinion, one important result of the present study is that superstorms appear to dissipate more of the transferred energy in the ring current rather than through ionospheric Joule heating.

It was found that threshold values of $B_z = -10$ nT, with peak values around -25 nT, during intervals greater than seven hours are the main criteria that causes super intense magnetic storms.

It is interesting that all the superstorms studied here occurred around the maximum phase of the solar cycle. Thus it would be interesting to consider geomagnetic superstorms occurring at solar minimum for a comparative study, since during such a phase of the solar cycle the storms could be associated to different solar and interplanetary sources with perhaps a different solar wind energy flux condition.

Table 9. Characteristic Values During Superstorm Main Phase

	Mean Power	Total Energy
Solar wind	2500 - 7000	7000 - 20,000
Magnetosphere	60 - 100	150 - 250
Ring current	15 - 25	40 - 60
Auroral ionosphere	11 - 14	26 - 36

Power in units of 10^{11} W; energy in units of 10^{15} J. $B_S \sim 25 - 30$ nT; $\Delta t \sim 7$ hours

Acknowledgments. We would like to thank B.T. Tsurutani, who kindly supplied interplanetary data, H. W. Kroehl, who provided ionospheric data and assistance when the first author was at NGDC/NOAA in Boulder, and T. J. Fuller-Rowell, who provided computed AMIE polar ionospheric electric potential and useful comments. We are also grateful to two referees for their careful reading of the original manuscript and helpful comments and suggestions.

The Editor thanks Y. Feldstein and another referee for their assistance in evaluating this paper.

References

Ahn, B. H., S. -I. Akasofu, and Y. Kamide, The Joule heat production rate and the particle energy injection rate as a funtion of the geomagnetic indices AE and AL, *J. Geophys. Res., 88*, 6275-6287, 1983.

Akasofu, S.-I., Energy coupling between the solar wind and the magnetosphere, *Space Sci. Res., 28*, 121-190, 1981.

Burton, R. K., R. L. McPherron, and C. T. Russell, An empirical relationship between interplanetary conditions and *Dst*, *J. Geophys. Res., 80*, 4204-4214, 1975.

Cole, K. D., Joule heating of the upper atmosphere, *Austr. J. Phys., 15*, 223, 1962.

Dessler, A. J., and E. N. Parker, Hydromagnetic theory of geomagnetic storms, *J. Geophys. Res., 64*, 2239-2252, 1959.

Feldstein, Y. I., Levitin, V. Pisarsky, A. Grafe, Ochabova, and A. Prigancová, Energy regimes in the Earth's magnetosphere, *Studia Geophys. Geod., 30*, 268-290, 1986.

Feldstein, Y. I., A. Grafe, V. Pisarskij, V. Yu., A. Prigancová, and P. V. Surnaruk, Magnetic field of the magnetospheric ring current and its dynamics during magnetic storms, *J. Atmos. Terr. Phys., 52*, 1185-1191, 1990.

Gonzalez, W. D., and F. S. Mozer, A quantitative model for the potential resulting from reconnection with an arbitrary interplanetary magnetic field, *J. Geophys. Res., 79*, 4186-4194, 1974.

Gonzalez, W. D., B. T. Tsurutani, A. L. C. Gonzalez, E. J. Smith, F. Tang, and S. -I. Akasofu, Solar wind-magnetosphere coupling during intense magnetic storms (1978-1979), *J. Geophys. Res., 94*, 8835-8851, 1989.

Gonzalez, W. D., J. A. Joselyn, Y. Kamide, H. W. Kroehl, G. Rostoker, B.T. Tsurutani, and V. W. Vasyliunas, What is a geomagnetic storm?, *J. Geophys. Res., 99*, 5771-5792, 1994.

Hewish, A., IPS - Imaging of disturbances in the inner heliosphere, *International Heliosphere Study, JPL*, 37-49, 1990

Holzer, R. E., and J. A. Slavin, Magnetic flux transfer associated with expansions and contractions of the dayside magnetosphere, *J. Geophys. Res., 83*, 3831, 1979.

Kroehl, H. W., J. F. McKee, K. R. Lutz, D. J. Gorney, and C. -I. Meng, A realistic model of high-latitude conductances produced by precipitating electrons, *Eos Trans. AGU, 69*, 1356, 1988.

Monreal-MacMahon, R., Energização global do sistema vento solar - magnetosfera - ionosfera durante tempestades magnéticas super intensas. Ph.D. dissertation, 168 pp., Instituto Nacional de Pesquisas Espaciais at São José dos Campos, June 1994.

Murayama, T., Coupling function between solar wind parameter and geomagnetic indices, *Rev. Geophys., 20*, 623-629, 1982.

Perrault, P., and S. -I. Akasofu, A study of geomagnetic storm, *Geophys. J. R. Astron. Soc. 54*, 547-573, 1978.

Prigancová, A., and Y. I. Feldstein, Magnetospheric storm dynamics in terms of energy output rate, *Planet. Space Sci., 40*, 581-588, 1992.

Reiff, P.H., and J. G. Luhmann, Solar wind control of the polar-cap voltage, in *Solar Wind - Magnetosphere Coupling* edited by Y. Kamide and J. A. Slavin, pp. 453-476, Terra Sci., Tokyo, 1986.

Sckopke, N., A general relation between the energy of trapped particles and the disturbance field near the Earth, *J. Geophys. Res., 71*, 3125-3130, 1966.

Sibeck, N., R. E. Lopez, and E. C. Roelof, Solar wind control of the magnetopause shape, location and motion, *J. Geophys. Res., 96*, 5489-5495, 1991.

Spreiter, J.R., A. L. Summers, and A. Y. Alksne, Hydrodynamics flow around the magnetosphere, *Planet. Space Sci., 14*, 223-253, 1966.

Stern, V.M., Energetics of the magnetosphere, *Space. Sci. Rev., 39*, 193-213, 1984.

Tsurutani, B. T., W. D. Gonzalez, F. Tang, and Y. T. Lee, Great magnetic storms, *Geophys. Res. Lett., 19*, 73-76, 1992.

Vasyliunas, V. M., J. R. Kan, G. L. Siscoe, and S.-I. Akasofu, Scaling relations governing magnetospheric energy transfer, *Planet. Space. Sci., 30*, 359-365, 1982.

Weiss, L. A., P. H. Reiff, J. J. Moses, B. D. Moore, and R. A. Heelis, Energy dissipation in substorms, *Eur. Space Agency Spec. Publ., ESA-SP-335*, 309-319, 1992.

W. D. Gonzalez, Divisão de Geofísica Espacial, Instituto de Pesquisas Espaciais, Caixa Postal 515,São José dos Campos, Brazil. (e-mail: gonzalez@dge.inpe.br)

R. A. Monreal Mac-Mahon, Departamento de Matemática y Física, Facultad de Ciencias, Universidad de Magallanes, Casilla 113-D, Punta Arenas, Chile. (e-mail: rmonreal@ona.fi.umag.cl)

(Received May 10, 1996; revised March 21, 1997; accepted April 14, 1997.)